PTEN regulates natural killer cell trafficking in vivo

Jeffrey W. Leong[a], Stephanie E. Schneider[a], Ryan P. Sullivan[a], Bijal A. Parikh[b], Bryan A. Anthony[a], Anvita Singh[a], Brea A. Jewell[a], Timothy Schappe[a], Julia A. Wagner[a], Daniel C. Link[a], Wayne M. Yokoyama[b], and Todd A. Fehniger[a,1]

Divisions of [a]Oncology and [b]Rheumatology, Department of Medicine, Washington University School of Medicine, St. Louis, MO 63110

Edited by Lewis L. Lanier, University of California, San Francisco, CA, and approved December 30, 2014 (received for review July 21, 2014)

Phosphatase and tensin homolog (PTEN) is a critical negative regulator of the phosphoinositide-3 kinase pathway, members of which play integral roles in natural killer (NK) cell development and function. However, the functions of PTEN in NK cell biology remain unknown. Here, we used an NK cell-specific PTEN-deletion mouse model to define the ramifications of intrinsic NK cell PTEN loss in vivo. In these mice, there was a significant defect in NK cell numbers in the bone marrow and peripheral organs despite increased proliferation and intact peripheral NK cell maturation. Unexpectedly, we observed a significant expansion of peripheral blood NK cells and the premature egress of NK cells from the bone marrow. The altered trafficking of NK cells from peripheral organs into the blood was due to selective hyperresponsiveness to the blood localizing chemokine S1P. To address the importance of this trafficking defect to NK cell immune responses, we investigated the ability of PTEN-deficient NK cells to traffic to a site of tumor challenge. PTEN-deficient NK cells were defective at migrating to distal tumor sites but were more effective at clearing tumors actively introduced into the peripheral blood. Collectively, these data identify PTEN as an essential regulator of NK cell localization in vivo during both homeostasis and malignancy.

cell migration | innate immunity | phosphatase | natural killer cell | PTEN

Natural killer (NK) cells are innate lymphoid cells critical for host defense against pathogens and antitumor responses (1–3). In the naïve mouse, NK cells are distributed among a number of hematopoietic and nonhematopoietic organs, including major reservoirs within the spleen, blood, and bone marrow (BM). Factors that orchestrate NK cell trafficking during homeostasis, including chemokine receptors and adhesion molecules, remain largely unknown. The majority of studies have focused on receptors controlling NK cell migration out of the BM, such as CXCR4 and $S1P_5$ (4–6). During inflammatory states, other receptors have defined roles for specific tissue homing, including CCR1, CCR5, CXCR3, CX3CR1, and CXCR6 (7). Integrin molecules, such as very late antigen-4 (VLA-4), also have specific functions in retaining NK cells within BM sinusoids (8). However, the downstream intracellular signaling pathways important for trafficking remain unclear, especially in light of the complex interplay of multiple chemotactic signals during an immune response.

One family of enzymes regulating a number of chemokine receptors includes the phosphoinositide 3-kinase (PI3K) signaling pathway, which plays a broad role in regulating cellular proliferation, gene expression, survival, cytoskeleton rearrangement, and migration (9). In immune cells, the PI3K pathway may be activated downstream of a number of receptors, including cytokine receptors and G protein-coupled receptors (GPCRs), the latter of which include most chemokine receptors. Stimulation of the PI3Ks results in the generation of phosphatidylinositol phosphate lipids, such as $PI(3,4,5)P_3$, and subsequent recruitment and activation of downstream signaling proteins, including Vav, Akt, and PDK1 (9, 10). Exogenous inhibition of PI3Ks suppresses perforin and granzyme B polarization and NK cell cytotoxicity (11). Additionally, deficiency of the leukocyte-selective PI3K p110γ or p110δ subunit results in defective NK cell development and maturation and alters the production of IFN gamma (IFN-γ) and cytotoxicity (12–14). New evidence has also linked IL-15 to the mammalian target of rapamycin (mTOR) pathway via PI3K activation (15, 16). Thus, PI3K signaling is a critical pathway for NK cell biological processes.

Two primary phosphatases oppose PI3K generation of the active secondary messenger $PI(3,4,5)P_3$: SH2-containing inositol-5′-phosphatase 1 (SHIP1) and phosphatase and tensin homolog (PTEN). SHIP1 specifically dephosphorylates $PI(3,4,5)P_3$ to $PI(3,4)P_2$, whereas PTEN dephosphorylates the 3′ inositol phosphate on $PI(3,4,5)P_3$, $PI(3,4)P_2$, and PI(3)P, thereby also counteracting other classes of PI3Ks (10). $SHIP1^{-/-}$ BM-chimeric mice have no overt alterations in NK cell distribution, and its intrinsic role in NK cell development only affects the terminal differentiation of mature NK cells (17). However, there are no reported studies of PTEN function in NK cells to date. The effects of lymphocyte-selective PTEN deficiency in T and B cells result from increased PI3K signaling and include increased cell survival and proliferation, lowered activation threshold through the B-cell receptor (18), and loss of costimulatory requirements in T cells (19). The role of phosphatases, particularly SHIP1 and PTEN, in cellular migration, however, remains controversial and appears to be dependent on both the cell studied and the mode of stimulation (20–22). Furthermore, unique aspects of PTEN function have been reported, including protein phosphatase activity (23) and regulation via intracellular sequestration to the cytoplasmic membrane (24). As PTEN is a major nonredundant regulator of PI3K signaling, we hypothesized that disruption of PI3K inhibition would uniquely impact NK cell developmental and functional pathways.

In this study, we generated NK cell-specific PTEN-deficient mice, which have diminished opposing lipid phosphatase activity to all known PI3K family members. PTEN-deficient mice display significant defects in peripheral organ and BM NK cell compartments, with a large proportion of NK cells being

Significance

Natural killer (NK) cells are critical players in the response to viruses and transformed cells, but the molecular mechanisms controlling their functions are incompletely understood. A major pathway leading to NK cell activation is the phosphoinositide 3-kinase pathway. However, the impact of phosphatase and tensin homolog (PTEN), a key phosphatase opposing this pathway, on NK cells has not been reported. We generated a previously unreported NK cell-intrinsic PTEN-deletion mouse model to evaluate its role in NK cell biology. In contrast to other lymphocytes, we demonstrate that the primary effects of PTEN loss are marked perturbation in NK cell trafficking and distribution during both homeostasis and malignancy. These findings indicate that PTEN plays an essential role in NK cell localization in vivo.

Author contributions: J.W.L. and T.A.F. designed research; J.W.L., S.E.S., R.P.S., B.A.P., B.A.A., A.S., B.A.J., T.S., and J.A.W. performed research; D.C.L. and W.M.Y. contributed new reagents/analytic tools; J.W.L. and T.A.F. analyzed data; and J.W.L. and T.A.F. wrote the paper.

The authors declare no conflict of interest.

This article is a PNAS Direct Submission.

[1]To whom correspondence should be addressed. Email: tfehnige@wustl.edu.

This article contains supporting information online at www.pnas.org/lookup/suppl/doi:10.1073/pnas.1413886112/-/DCSupplemental.

inappropriately localized to the blood. These effects were due in part to alterations in NK cell trafficking in vivo, a defect that also prevented their recruitment to a localized tumor challenge. These results identify a previously unidentified role for PTEN in regulating NK cell tissue distribution during both homeostasis and malignancy in vivo.

Results

NK Cell-Specific PTEN Deletion Alters Steady-State Tissue Distribution. To identify NK cell-specific alterations within hematopoietic compartments, we generated Ncr1KI-iCre (25) × ROSA26KI-YFP$^{loxP/stop/loxP}$ mice (hereafter referred to as PTEN$^{+/+}$) and combined these alleles with PTEN$^{flox/flox}$ (26) (hereafter referred to as PTEN$^{\Delta/\Delta}$). In these mice, the expression of *Ncr1*/NKp46 leads to Cre-mediated excision of the phosphatase domain of *pten* (exon 5) and coexpression of the YFP reporter allele (Fig. S1*A*). Loss of exon 5 was confirmed by RT-PCR analysis in PTEN$^{\Delta/\Delta}$ YFP^{+} NK cells (Fig. S1*B*). As reported previously, we observed that >99% of NKp46^{+} NK cells in PTEN$^{+/+}$ and PTEN$^{\Delta/\Delta}$ mice were YFP^{+} (25). Additionally, in line with PTEN excision in other hematopoietic cells (18, 26), we did not detect PTEN protein expression following Cre-mediated excision (Fig. S1*C*).

PTEN$^{\Delta/\Delta}$ NK cells were abnormally distributed among typical NK cell compartments, with decreased NK cell percentages in the spleen, liver, lymph node (LN), and BM (Fig. 1 *A* and *B*). In contrast, NK cell percentages were significantly increased in the blood and lung, suggesting a defective localization of NK cells to typical NK cell reservoirs in vivo. We further confirmed these findings with a second NK-specific Cre model (27) (Ncr1-tg iCre × ROSA26-KI × YFP$^{lox/stop/lox}$ PTEN$^{\Delta/\Delta}$ mice), which demonstrated similar alterations in NK cell distribution (Fig. S1*D*). To assess changes in NK cell compartments on a whole organism level, we compared the absolute NK cell numbers in PTEN$^{+/+}$ and PTEN$^{\Delta/\Delta}$ mice, taking into account total changes within the BM space, secondary lymphoid tissue, and intravascular volume (Fig. 1*C*). Despite a significant increase in blood NK cells, PTEN$^{\Delta/\Delta}$ mice remained deficient overall in NK cells (Fig. 1*D*). Examination of PTEN$^{\Delta/\Delta}$ spleen and BM immunosections revealed no gross abnormalities in NK cell localization within these organs (Fig. S1 *E* and *F*). Based on this NK cell distribution phenotype, we hypothesized that several nonmutually exclusive possibilities may be occurring with PTEN deficiency: (*i*) a defect in NK cell development within the BM, (*ii*) altered NK cell proliferation, (*iii*) increased retention of NK cells within the blood, (*iv*) acquired homing of mature NK cells to the lung, and (*v*) augmented egress of NK cells from the BM and LNs.

PTEN Deficiency Alters the CD27/CD11b Maturation Frequency Specifically in the BM and LN. NK cell movement from the BM into the periphery is normally influenced by maturation, as evidenced by observations that the BM is predominately composed of stage II and III NK cells, whereas peripheral tissues contain mostly stage IV NK cells (28). To determine whether the distribution of NK cells was reflective of altered maturation, we analyzed CD27/CD11b NK cell maturation stages. PTEN$^{\Delta/\Delta}$ NK cells had a significantly higher frequency of stage II NK cells in the

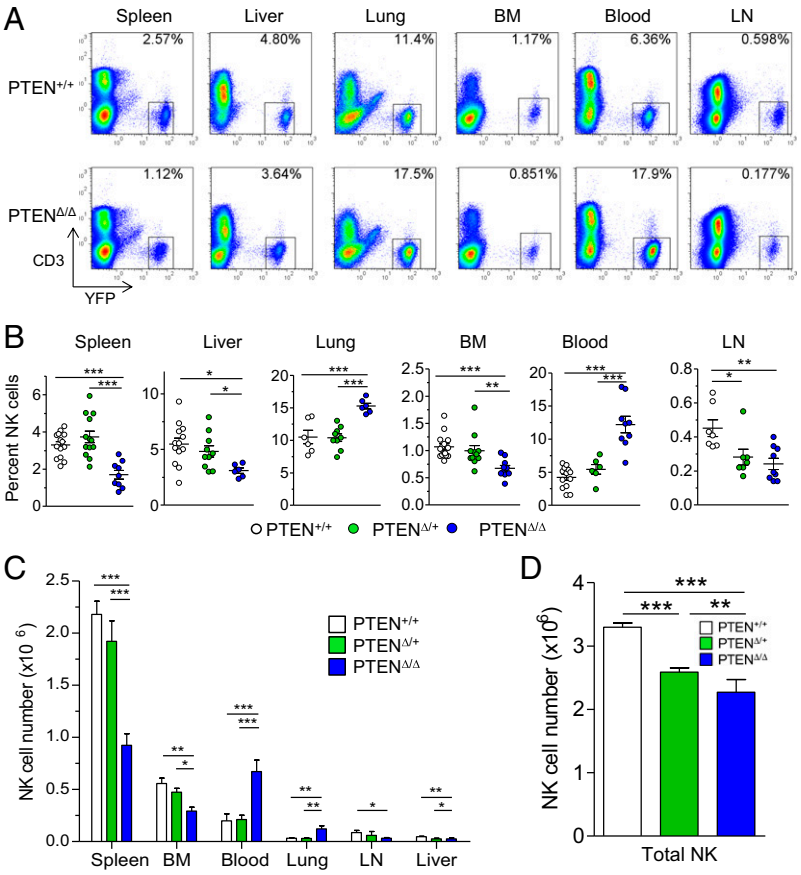

Fig. 1. NK cell-specific PTEN deletion results in the altered in vivo distribution of NK cells. (*A*) Representative bivariate flow cytometric plots pregated on lymphocytes from the indicated organs of PTEN$^{+/+}$ or PTEN$^{\Delta/\Delta}$ mice. (*B*) Summary data of NK cell percentages of gated lymphocytes from various organs, with each data point representing an individual mouse. (*C*) Absolute NK cell numbers within each organ was calculated taking into account the total organ space, as described in *Materials and Methods*. (*D*) Total NK cells per individual mouse were calculated by summation of NK cell numbers in *C*. Data are mean ± SEM of eight independent experiments using a total of 5–15 mice per genotype.

BM (albeit to a modest degree) and a considerably higher frequency of stage IV NK cells in the LNs, compared with control mice (Fig. 2*A*). Despite this change in NK cell subset frequency in these organs, we still observed decreased numbers of NK cells in these subsets (Fig. 2*B*). Surprisingly, NK cells were of near equivalent maturity elsewhere, including organs in which NK cells were deficient—the spleen and liver—and organs in which NK cells were expanded—the lung and blood. The total number of each PTEN$^{\Delta/\Delta}$ NK cell maturation subset was proportionally reduced in these organs compared with PTEN$^{+/+}$ NK cells (Fig. 2*B*). Although we observed a higher percentage of stage II NK cells in PTEN$^{\Delta/\Delta}$ BM, we reasoned that a block in maturation was unlikely based on the lack of accumulation of undifferentiated precursor NK cells (Fig. 2*B*). Furthermore, NK cell precursor (Lin$^-$ CD122$^+$ NK1.1$^-$) frequency and numbers were unaltered and thus were not responsible for decreased immature NK cell numbers (Fig. S1*G*). Thus, with the exception of the BM and LNs, PTEN deficiency causes the altered distribution of NK cells independent of maturation status.

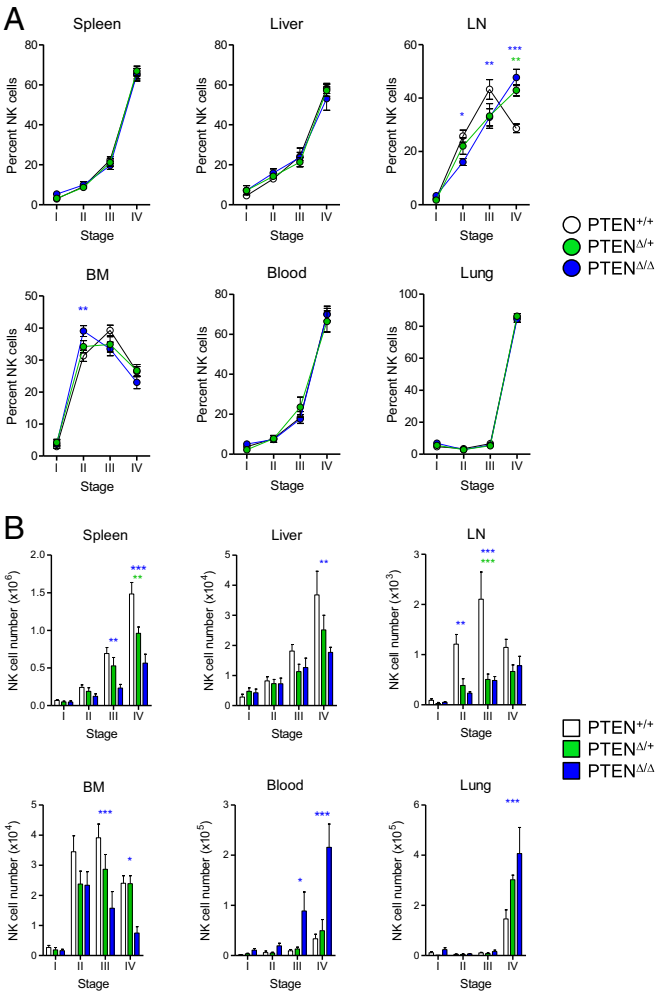

Fig. 2. Peripheral NK cell deficiency with PTEN loss is not a result of maturation differences. (*A*) The maturation of YFP$^+$ NK cells in various organs was analyzed by flow cytometric expression of CD27 and CD11b expression. Maturation stages were identified as follows: stage I, CD27$^-$CD11b$^-$; stage II, CD27$^+$CD11b$^-$; stage III, CD27$^+$CD11b$^+$; stage IV, CD27$^-$CD11b$^+$. (*B*) Total organ cell numbers were calculated by multiplying percentages of maturation stages by the total number of NK cells within each organ. For certain organs, the total NK cells are shown as the total per femur (BM), total per inguinal LN pair, and the total per mL (blood). Data shown are mean ± SEM of at least three independent experiments including 8–14 mice per organ. Significance is indicated above each maturation stage comparing PTEN$^{\Delta/\Delta}$ (blue) or PTEN$^{\Delta/+}$ (green) to PTEN$^{+/+}$.

PTEN$^{\Delta/\Delta}$ NK Cells Display Alterations in Receptor Expression, Functionality, and PI3K Signaling. We assessed a number of maturation markers and activating and inhibitory receptors to definitively characterize the role of PTEN in NK cell maturation. In line with the expanded stage II NK cell frequency in PTEN$^{\Delta/\Delta}$ BM, we found increased CD51 expression and decreased CD43 expression (Fig. S1*H*). However, we found no differences in CD122, NK1.1, or NKp46 expression (Fig. S1*I*). PTEN$^{\Delta/\Delta}$ splenic NK cells displayed modest alterations in Ly49 and NKG2A/C/E receptor expression (Fig. S1*J*), suggesting that PTEN may regulate the acquisition of these receptors or the maintenance of these subsets. Thus, the terminal maturation of NK cells is modestly affected by PTEN deletion. As the PI3K pathway is known to be a major route for NK cell activation, we also evaluated the expression of CD69 but found no difference between PTEN$^{+/+}$ and PTEN$^{\Delta/\Delta}$ NK cells (Fig. S1*K*). We additionally investigated altered NK cell functionality but were surprised to find less IFN-γ production in response to cytokine combinations such as IL-12 + IL-15 or IL-12 + IL-18 compared with control NK cells (Fig. S2). These data suggest that PTEN selectively promotes cytokine-triggered IFN-γ production, as PTEN$^{\Delta/\Delta}$ NK cells produced equivalent IFN-γ and degranulated similarly to control NK cells if stimulated through NK1.1 (Fig. S2).

We next investigated whether the absence of PTEN results in enhanced PI3K activity in NK cells. We assessed the phosphorylation of AKT, a downstream target of the PI3K pathway, both at baseline and after stimulation with IL-15, a cytokine known to signal through AKT and mTOR (16). Although we did not detect increased basal p-AKT expression, we observed enhanced p-AKT following IL-15 stimulation (Fig. S3 *A–C*) and increased phosphorylation of the mTOR substrates 4E-BP1 and S6 kinase (Fig. S3 *D* and *E*) at baseline. mTOR activation in PTEN$^{\Delta/\Delta}$ NK cells was significantly increased following IL-15 stimulation but not NK1.1 ligation, consistent with a previous report demonstrating an absence of mTOR induction by activating receptor engagement (16). In summary, the deletion of PTEN results in augmented PI3K pathway activation, particularly after IL-15 stimulation.

PTEN Deficiency Increases NK Cell Turnover. To assess whether the reduction of NK cells in peripheral organs reflected the altered proliferation or survival of NK cells, we examined rates of apoptosis, BrdU incorporation, and K_i-67 expression. We found moderate decreases in the viability of PTEN$^{\Delta/\Delta}$ NK cells derived from the BM and a trend toward increased splenic NK cell death, but no change in the viability of NK cells from the peripheral blood (Fig. 3*A*). These data were consistent with the observed increase in caspase activation observed in BM NK cells (Fig. S4*A*). Conversely, PTEN$^{\Delta/\Delta}$ NK cells had significantly more BrdU incorporation over a 3-d period and increased expression of K_i-67, indicating that the loss of PTEN results in greatly increased proliferation (Fig. 3*B*). This enhanced proliferation was independent of maturation stage (Fig. S5). Interestingly, we were unable to see increased cell death of PTEN$^{\Delta/\Delta}$ NK cells when cultured ex vivo in limiting doses of IL-15 (Fig. S4*B*). Taken together with the modest overall net decrease in total body NK cell numbers, these data seem paradoxical—the amount of proliferation appeared to outweigh that of cell death.

To ensure that our readout of PTEN$^{\Delta/\Delta}$ NK cell death was not influenced by experimental variability of different mice, we generated mixed BM chimeras to better compare PTEN$^{+/+}$ and PTEN$^{\Delta/\Delta}$ NK cells in a competitive environment within the same mouse (Fig. 3*C*). We confirmed that PTEN$^{\Delta/\Delta}$ NK cells are relocalized to the peripheral blood and lung from other lymphoid organs and

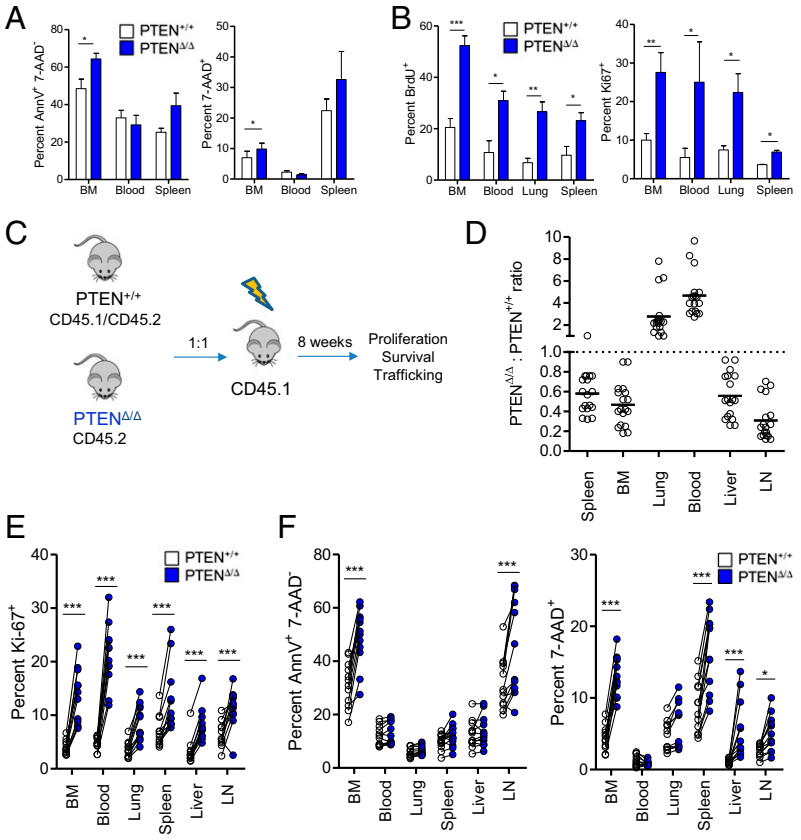

Fig. 3. PTEN$^{\Delta/\Delta}$ NK cells have increased cellular proliferation and reduced survival in vivo. (*A*) The survival of NK1.1^{+} NKp46^{+} CD3^{-} NK cells in various organs was evaluated by flow cytometric analysis of annexin V (AnnV) and 7-AAD labeling. Data shown are mean ± SEM, representing four mice of each genotype, performed in three independent experiments. (*B*) Flow cytometric analysis of BrdU incorporation in YFP^{+} CD3^{-} cells following 3 d, with every 12-h i.p. injection of BrdU or Ki-67 staining of untreated mice. Data shown are mean ± SEM, representing four mice of each genotype in two independent experiments. (*C*) Competitive mixed BM chimeras were generated using a 1:1 mix of whole BM from PTEN$^{+/+}$ and PTEN$^{\Delta/\Delta}$ mice. Organs were analyzed at 8 wk for (*D*) NK cell distribution, (*E*) proliferation, and (*F*) death. Each point in *D* represents an individual mouse, with a total of 18 mice from three biological replicate groups. Two of these groups were further analyzed for proliferation and survival in *E* and *F*. Each line connects the positive staining population from PTEN$^{+/+}$ and PTEN$^{\Delta/\Delta}$ donor NK cells within the same mouse.

have greatly increased proliferation (Fig. 3 *D* and *E*). However, these experiments also revealed a significant increase in cell death in PTEN$^{\Delta/\Delta}$ NK cells. These data suggest that our measurements of apoptosis and cell death comparing different control and PTEN$^{\Delta/\Delta}$ mice were underestimating the increases in cell death of PTEN$^{\Delta/\Delta}$ NK cells. Indeed, we observed that although the percentages of PTEN$^{+/+}$ and PTEN$^{\Delta/\Delta}$ NK cell death varied between chimeric mice (even within the same experiment), there was a consistent and reproducible increase in NK cell death within the same mouse, particularly in the spleen, BM, liver, and LN, but not in the lung or blood (Fig. 3*F*). Taken together, the increased NK cell proliferation in all organs, increased cell death in most lymphoid organs, and the lack of cell death in the blood and lung likely contributed to the altered distribution of NK cells in PTEN$^{\Delta/\Delta}$ mice.

Abnormal Retention of NK Cells Contributes to the Elevated Peripheral Blood Pool. We further questioned whether alterations in NK cell retention and trafficking could contribute to the increased peripheral blood NK cell numbers. We used a short-term competitive transfer model in which blood NK cells of mixed genotypes were injected intravascularly into the same wild-type recipient at an equal ratio (Fig. 4*A*). After 16 h, a time sufficient to achieve steady-state distribution, we examined changes in the relative distribution of donor NK cells. Blood-resident PTEN$^{\Delta/\Delta}$ NK cells were significantly impaired in their recruitment to the BM, liver, and spleen, but preferentially resided in the peripheral blood and lung (Fig. 4 *B* and *C*). Similar trafficking defects were seen when using spleen or BM donor NK cells, suggesting that an intrinsic defect in PTEN$^{\Delta/\Delta}$ NK cells, independent of organ residence, was responsible for their blood retention (Fig. 4*C*). Furthermore, we found similar maturation profiles of control and PTEN$^{\Delta/\Delta}$ NK cells in the blood, spleen, and lung following transfer (Fig. S6 *A* and *B*), consistent with the lack of maturation differences in the majority of lymphoid organs in control and PTEN$^{\Delta/\Delta}$ mice. The trafficking of PTEN$^{\Delta/+}$ NK cells had modest, but nonsignificant, defects in homing to peripheral organs (Fig. S6*C*).

Intriguingly, PTEN$^{\Delta/\Delta}$ NK cells within the lung were also elevated. To assess whether the increase in lung NK cells in PTEN$^{\Delta/\Delta}$ mice was truly a homing phenomenon or simply a reflection of increased peripheral blood NK cells, we examined whether there was an increase in lung parenchyma-infiltrating NK cells. We differentiated parenchymal (lung-resident) versus vascular-associated NK cells by specifically labeling intravascular cells with short-term i.v. anti-CD45 antibody as previously described (4, 29). PTEN$^{+/+}$ NK cells were exclusively labeled with i.v. anti-CD45, indicating that wild-type lung NK cells are normally localized completely within the lung vasculature (Fig. S7*A*). We did not observe an increase in lung-infiltrating NK cells in PTEN$^{\Delta/\Delta}$ mice, as PTEN$^{\Delta/\Delta}$ NK cells were also fully labeled with anti-CD45 antibody. Thus, these data suggest that the increase in lung NK cells in PTEN$^{\Delta/\Delta}$ mice is reflective of the elevated peripheral blood NK cell numbers.

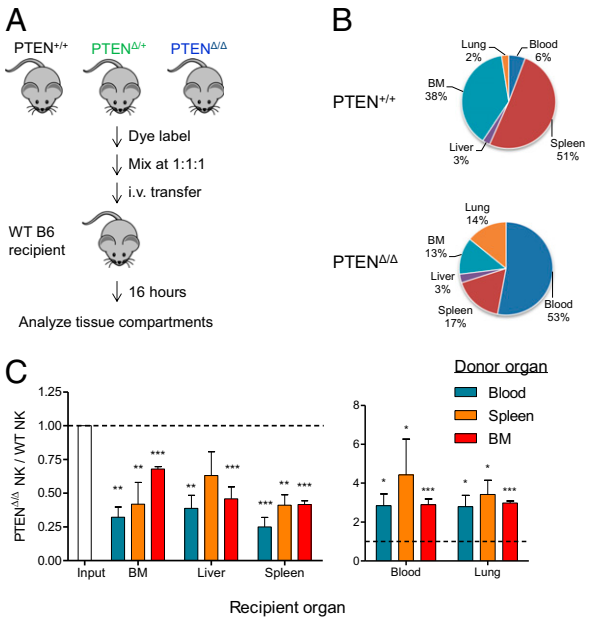

Fig. 4. Elevated NK cell retention in the blood contributes to the NK cell redistribution observed in PTEN$^{\Delta/\Delta}$ mice. (*A*) Blood mononuclear cells or total splenocytes were isolated, individually dye labeled, and mixed such that YFP^{+} NK cells were at equal cell ratios (~1:1:1). Cell mixtures were i.v. transferred into wild-type recipients and killed after 16 h. (*B*) The relative distribution among organs of donor PTEN$^{+/+}$ or PTEN$^{\Delta/\Delta}$ NK cells within a representative wild-type recipient after adoptive transfer. (*C*) Various organs were isolated following adoptive transfer, and the ratio of donor PTEN$^{\Delta/\Delta}$ (shown here) or PTEN$^{\Delta/+}$ (shown in Fig. S6*C*) to PTEN$^{+/+}$ NK cells was calculated. Significance is indicated compared with PTEN$^{+/+}$ NK cells. Data shown are mean ± SEM of four independent experiments using one mouse per genotype per experiment.

In contrast, other lymphoid organs known to be highly vascularized similar to the lung, such as the liver, did not show increased NK cell numbers in PTEN$^{\Delta/\Delta}$ mice. We hypothesized that due to our use of cardiac puncture removal of peripheral blood, we were likely removing the peripheral blood NK cell component of the liver but not the lung, which uniquely contains a large network of branching microvasculature. Indeed, we found no difference in lung NK cell frequency after cardiac puncture removal of peripheral blood, even with additional saline perfusion of the lung vasculature (Fig. S7*B*). These data suggest that the majority of lung NK cells are likely marginated to vessel walls, consistent with reports concerning lung lymphocytes (30, 31). In contrast, we observed a far greater liver NK cell deficiency in PTEN$^{\Delta/\Delta}$ mice following cardiac puncture removal of peripheral blood, suggesting that the peripheral blood component of PTEN$^{\Delta/\Delta}$ liver is greatly expanded (Fig. S7*C*). Thus, the blood NK cell pool in both the liver and lung is increased in PTEN$^{\Delta/\Delta}$ mice but is effectively removed by cardiac puncture in the liver and not the lung.

PTEN-Deficient NK Cells Prematurely Exit the BM. We next investigated whether altered exit from the BM was a contributing mechanism for blood accumulation in PTEN-deficient NK cells. We examined parenchymal (BM tissue-resident) versus sinusoidal (vascular-associated) BM NK cells by specifically labeling sinusoidal BM cells using the i.v. anti-CD45 antibody described earlier. In this assay, cells within sinusoids are accessible to circulating CD45 antibody and are consequently stained, whereas nonvascular (parenchymal) NK cells fail to stain in the 5-min assay. In contrast to blood NK cells, we observed enhanced egress from the BM (Fig. 5 *A* and *B*). PTEN$^{\Delta/\Delta}$ NK cells were redistributed from the BM parenchyma to the sinusoids, an effect observed across all NK cell maturation subsets (Fig. 5*C*).

Although there were no changes in CD27/CD11b subset percentages within the parenchyma, stage II, III, and IV NK cells were all significantly reduced in number in PTEN$^{\Delta/\Delta}$ mice (Fig. 5*D*). Examination of the sinusoidal fraction, however, did not reveal a parallel increase in stage II–IV NK cell numbers. Instead, there was no proportional change in stage II and III and in fact a decrease in sinusoidal stage IV NK cells, the primary constituent of BM sinusoids (Fig. 5*D*). The lack of a significant increase in sinusoidal NK cells likely reflects simultaneous loss of retention within both the parenchyma and sinusoids, resulting in exit from the BM. This hypothesis was supported by the elevated NK cell numbers in the blood, especially the stage IV NK cells (Fig. 2*B*). Indeed, PTEN$^{\Delta/\Delta}$ mice with a comparable percentage of sinusoidal NK cells to PTEN$^{+/+}$ mice exhibited a parallel loss of the stage IV sinusoidal NK cells, also consistent with more rapid exit to the blood (Fig. 5*E*). Thus, a change in localization of NK cells from the parenchyma to the sinusoids, in addition to more pronounced exit from the sinusoids, contributes to changes in the maturation profile of BM NK cells and mirrors NK cell increases in the blood.

BM retention of developing NK cells is highly dependent on chemokine gradients and integrin interactions that either recruit or prevent NK cell migration. CXCL12 and VCAM-1 both have important roles in the retention of BM NK cells by binding to CXCR4 and VLA-4 on NK cells, respectively (4, 8). Engagement

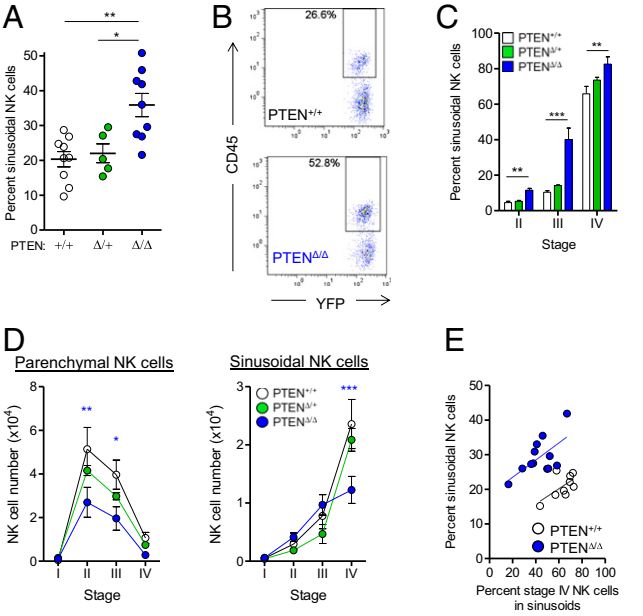

Fig. 5. PTEN$^{\Delta/\Delta}$ mice have increased NK cell egress from the BM. Parenchymal and sinusoidal NK cells in the BM were assessed using short-term injection of fluorophore-conjugated anti-CD45 antibody to label the intravascular accessible BM space. (*A*) BM PTEN$^{\Delta/\Delta}$ NK cells are preferentially found within the sinusoids (CD45-labeled fraction). (*B*) Representative bivariate plots of increased CD45 labeling in PTEN$^{\Delta/\Delta}$ NK cells. (*C*) Increased CD45^{+} PTEN$^{\Delta/\Delta}$ NK cells were observed in all maturation stages, as defined by CD27 and CD11b expression. (*D*) CD45-unlabeled (parenchymal) and CD45-labeled (sinusoidal) fractions were analyzed for cell numbers within each stage. (*E*) The relatively normal BM sinusoidal fraction in some PTEN$^{\Delta/\Delta}$ mice is due to accelerated loss of stage IV NK cells. The percentage of sinusoidal NK cells is shown plotted against the percentage of stage IV NK cells within the sinusoids of each mouse. Data shown in *A*–*D* are mean ± SEM of at least three independent experiments using nine PTEN$^{+/+}$, five PTEN$^{\Delta/+}$, and nine PTEN$^{\Delta/\Delta}$ mice. (*E*) Mean ± SEM of eight PTEN$^{+/+}$ and 12 PTEN$^{\Delta/\Delta}$ mice of at least three independent experiments.

of these receptors can trigger activation of the PI3K pathway (32, 33). To test whether insufficient chemokine or integrin retention signals could explain the loss of BM NK cells, we treated PTEN$^{+/+}$ or PTEN$^{\Delta/\Delta}$ mice with the CXCR4 antagonist AMD3100 or the VLA-4 inhibitor firategrast. In control mice, treatment with AMD3100 or firategrast promoted exit of NK cells from the BM (Fig. S8*A*). However, PTEN$^{\Delta/\Delta}$ NK cells had no further depletion after treatment with these inhibitors individually and were similar to the BM compartment of inhibitor-treated PTEN$^{+/+}$ mice. Interestingly, we observed no increase in blood NK cell numbers even in PTEN$^{+/+}$ mice when AMD3100 or firategrast was used alone, which may reflect mobilization to other lymphoid organs, as is known to occur in mice treated with AMD3100 (34). Nevertheless, treatment with AMD3100 and firategrast together promoted substantial release of PTEN$^{+/+}$ NK cells from the BM and parallel increases in peripheral blood NK cell number, thus phenocopying PTEN$^{\Delta/\Delta}$ mice (Fig. S8*B*). Thus, PTEN$^{\Delta/\Delta}$ NK cells have an apparent insensitivity to BM retention signals.

PTEN Deficiency Alters LN Constituency. Similar to the BM, we observed alterations in the maturation profile of PTEN$^{\Delta/\Delta}$ NK cells within LNs (Fig. 2*A*). Immunofluorescence staining of PTEN$^{\Delta/\Delta}$ LN sections revealed substantial increases in NK cell frequency within nonfollicular regions, whereas PTEN$^{+/+}$ NK cells were also found in the paracortex (Fig. 6*A*). We hypothesized that this change in localization could reflect preferential residence in cortical sinuses. Therefore, we analyzed the LN NK cell distribution using short-term anti-CD45 labeling, which has been previously shown to differentiate NK cells within the parenchyma and draining cortical and medullary sinuses (4). We observed a significant increase in the fraction of PTEN$^{\Delta/\Delta}$ NK cells distributed into sinuses across all maturation subsets (Fig. 6 *B* and *C*). Further examination of the parenchymal and sinusoidal compartments revealed that although the relative distribution of maturation subsets was intact in either compartment, the parenchyma was deficient in NK cells, whereas the sinuses were relatively unchanged in NK cell number (Fig. 6*D*). These data suggest that in the absence of PTEN, a large proportion of NK cells in the LN are relocated to exiting sinuses, rather than entering and transiently migrating through the paracortex and medulla of the LN as reported previously for wild-type NK cells (35–37). We further questioned whether defects in parenchymal entry could also be due to altered surface expression of CD62L, a selectin essential for NK cell entry into the LN (38). As shown in Fig. 6*E*, we found significantly less CD62L expression in PTEN$^{\Delta/\Delta}$ NK cells. This reduced CD62L expression likely contributes to reduced LN homing in PTEN$^{\Delta/\Delta}$ mice.

PTEN$^{\Delta/\Delta}$ NK Cells Are Specifically Hyperresponsive to S1P Signals and Express Increased Integrin Receptor Density. Given the apparent insensitivity of PTEN$^{\Delta/\Delta}$ NK cells to CXCR4 antagonists in vivo, we questioned whether responses to CXCL12 in vitro would be diminished. Surprisingly, we observed no defects in the migration of NK cells from the BM, blood, or spleen across transwells in response to CXCL12 (Fig. 7*A*). Furthermore, we examined the expression of CXCR4, as well as a panel of known chemokine and integrin receptors involved in NK cell trafficking, and found no changes in CXCR4 or other chemokine receptor expression (Fig. S9). However, we observed significantly increased expression of the integrin receptors CD49d and the ICAM-1 receptor LFA-1. Migration of PTEN$^{\Delta/\Delta}$ NK cells across ICAM-1–coated transwells was impaired, and although this may contribute to defects in peripheral blood egress, it does not explain increased BM NK cell exit (Fig. S8*C*).

We postulated that overriding sensitivity to specific chemokines could result in an apparent insensitivity of NK cells to retention signals such as CXCR4 and VLA-4. We evaluated the chemotaxis of PTEN$^{\Delta/\Delta}$ NK cells to known NK cell-recruiting

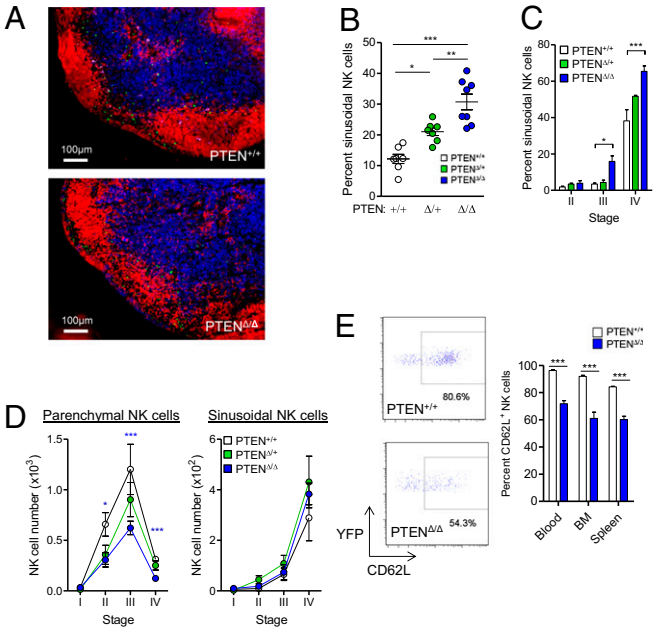

Fig. 6. The maturation defects and NK cell deficiency in PTEN$^{\Delta/\Delta}$ LNs can be attributed to decreased NK cell retention and CD62L expression. (*A*) Immunosections of PTEN$^{+/+}$ or PTEN$^{\Delta/\Delta}$ inguinal LNs stained for NK cells (YFP, green), B220 (red), and CD3 (blue). Representative images of inguinal LNs from two mice are shown. (*B–D*) PTEN$^{+/+}$ or PTEN$^{\Delta/\Delta}$ mice were injected with anti-CD45 antibody and killed after 5 min. Both inguinal LNs were removed and analyzed for CD45-unlabeled (parenchymal) or CD45-labeled (sinusoidal) fractions on YFP^{+}-gated NK populations. (*B*) CD45-labeled LN NK cells are increased in PTEN$^{\Delta/\Delta}$ mice. (*C*) Redistribution to LN sinuses was observed in maturation stages III and IV. LN NK cells were stained for CD27/CD11b maturation stages and further subdivided by CD45-unlabeled and CD45-labeled cells. (*D*) The abnormally increased sinusoidal NK cell numbers in the LNs are associated with decreased parenchymal NK cells. CD45^{-} and CD45^{+} fractions were analyzed for NK cell numbers within each maturation stage. (*E*) A significant proportion of PTEN$^{\Delta/\Delta}$ NK cells have decreased CD62L expression. A representative flow cytometry plot of splenic NK cells is shown. Summary of mean ± SEM percent CD62L^{+} NK cells from four to 11 mice per organ. (*B–D*) Mean ± SEM of seven independent experiments including seven PTEN$^{+/+}$, seven PTEN$^{\Delta/+}$, and eight PTEN$^{\Delta/\Delta}$ mice.

chemokines, such as CCL2, CCL3, and CXCL10, but found no difference in their migration (Fig. S8*D*). However, chemotaxis to S1P was specifically enhanced in PTEN$^{\Delta/\Delta}$ NK cells and was most evident in NK cells derived from the peripheral blood, which typically display insensitivity to S1P to allow egress into peripheral tissues (Fig. 7*B*). Because of the low overall migration to S1P, we assessed the chemotaxis of PTEN$^{+/+}$ and PTEN$^{\Delta/\Delta}$ NK cells independently and in a competitive fashion (shown in Fig. 7*B*) using equivalent numbers of NK cells in the same transwell. These experiments revealed significantly increased migration in response to S1P by PTEN$^{\Delta/\Delta}$ NK cells.

We did not detect changes in S1P5 transcript levels (Fig. 7*C*), suggesting that PTEN likely regulates pathways downstream of $S1P_5$. Therefore, we assessed signaling changes following S1P stimulation in PTEN$^{+/+}$ and PTEN$^{\Delta/\Delta}$ NK cells. $S1P_5$ is known to couple to $G\alpha_{i/0}$ (signaling through PI3K/AKT and MAPK) and $G\alpha_{12/13}$, the signaling of which likely activates multiple pathways, including PI3K/AKT, RhoA/ROCK, and RasGAP, leading to down-regulation of ERK (39, 40). Stimulation of PTEN$^{+/+}$ NK cells with S1P leads to transient down-regulation of p-ERK (Fig. 7*E*, solid lines). Surprisingly, we found that a majority of freshly isolated PTEN$^{\Delta/\Delta}$ NK cells expressed nonphosphorylated ERK at baseline (Fig. 7 *D* and *E*). Correspondingly, the $S1P_5$ receptor has been shown to intrinsically down-regulate ERK activity in

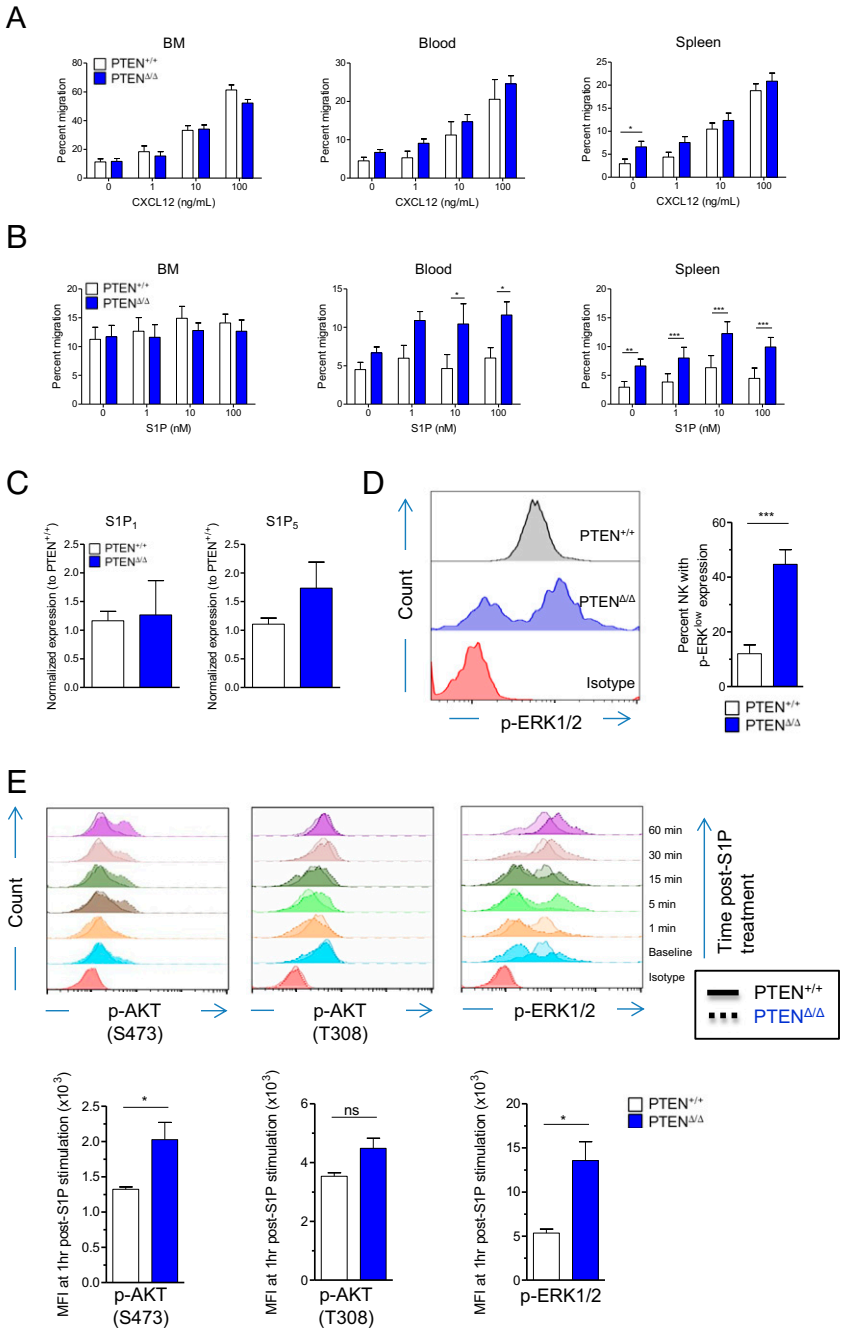

Fig. 7. PTEN$^{\Delta/\Delta}$ NK cells have enhanced migration to S1P and display signaling alterations to S1P stimulation in vitro. In vitro migration transwell assays of NK cells from various organs against (*A*) CXCL12 or (*B*) S1P show enhanced PTEN$^{\Delta/\Delta}$ NK cell chemotaxis to S1P. (*C*) S1PR1 and S1PR5 mRNA is similarly expressed in PTEN$^{+/+}$ and PTEN$^{\Delta/\Delta}$ FACS-purified splenic NK cells by real-time PCR. (*D*) A significant fraction of freshly isolated PTEN$^{\Delta/\Delta}$ NK cells exhibit decreased ERK phosphorylation without exogenous S1P stimulation. (*E*) Enhanced phosphorylation of AKT and ERK during stimulation of PTEN$^{\Delta/\Delta}$ (dashed line) compared with PTEN$^{+/+}$ (solid line) splenic NK cells with S1P in vitro. Summary data in *A* and *B* are mean ± SEM summarizing four mice in four independent experiments. Data in *C* are mean ± SEM from three mice and in *D* and *E* are mean ± SEM from three mice in three independent experiments.

the absence of ligand (41). We predict that this alteration in ERK activity is likely related to S1P conditioning in vivo. Following S1P stimulation for 1 h, we found increased phosphorylation of both AKT (S473) and ERK on PTEN$^{\Delta/\Delta}$ NK cells (Fig. 7*E*), again correlating with the increased migration against S1P gradients. Thus, these data connect PTEN and overactive S1P signaling as a mechanism behind increased blood NK cell redistribution.

Impaired Trafficking of PTEN$^{\Delta/\Delta}$ NK Cells to Tumor Sites in Vivo. NK cell antitumor responses depend on their ability to traffic to sites of malignant transformation. To evaluate whether PTEN$^{\Delta/\Delta}$ NK cells could mount an active NK cell response to malignancy despite their steady-state localization defect, we used a syngeneic tumor model in which the RMA and RMA/S lymphoma cell lines were coinjected intraperitoneally (i.p.) into PTEN$^{+/+}$ or PTEN$^{\Delta/\Delta}$ mice. Although we initially designed these experiments to potentially analyze NK cell-mediated tumor clearance via the selective elimination of NK cell-sensitive RMA/S cells, we observed minimal clearance of RMA/S by wild-type NK cells, likely due to the marked outnumbering of the NK cells by tumor cells

in this model. Expansion of the peritoneal NK cell pool was assessed 24 and 48 h after RMA:RMA/S challenge. Similar to other lymphoid organs in the setting of PTEN deficiency, there were significantly fewer PTEN$^{\Delta/\Delta}$ NK cells in the peritoneum during homeostasis (Fig. 8*A*). Following injection of control or PTEN$^{\Delta/\Delta}$ mice with RMA:RMA/S i.p., we found decreased peritoneal NK cell numbers in the PTEN$^{\Delta/\Delta}$ mice compared with controls (Fig. 8*B*). However, we observed a modest increase in PTEN$^{\Delta/\Delta}$ NK cells in the peritoneal cavity, likely due to enhanced proliferation (Fig. 3) of existing PTEN$^{\Delta/\Delta}$ NK cells in the peritoneum.

To more definitively evaluate the requirement for PTEN in the recruitment of NK cells into the peritoneum, we adoptively transferred enriched PTEN$^{+/+}$ or PTEN$^{\Delta/\Delta}$ NK cells i.v. into syngeneic recipient Rag2$^{-/-}\gamma_c{}^{-/-}$ mice that lacked endogenous NK cells. We concurrently transferred RMA:RMA/S cells i.p. (Fig. 8*C*). Without tumor challenge, both PTEN$^{+/+}$ or PTEN$^{\Delta/\Delta}$ NK cells failed to traffic to the peritoneum. However, in mice challenged with RMA:RMA/S tumor, only PTEN$^{+/+}$ NK cells were capable of trafficking to the peritoneum from the blood.

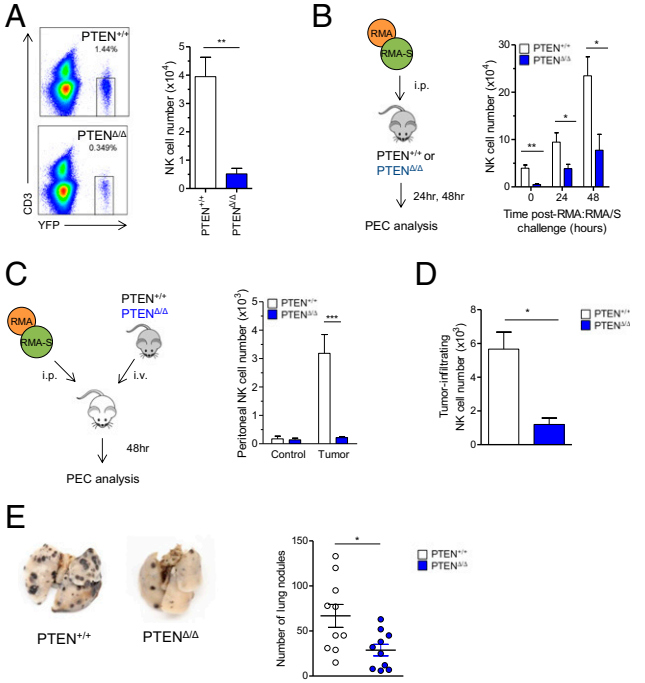

Fig. 8. PTEN-deficient NK cells are unable to migrate to distant sites of tumor challenge. (*A*) The peritoneal cavity of PTEN$^{\Delta/\Delta}$ mice is deficient in NK cells at steady state. Shown are representative bivariate plots of single cell suspensions generated from the flushed peritoneal cavity of PTEN$^{+/+}$ or PTEN$^{\Delta/\Delta}$ mice and summary data showing mean ± SEM of 3–4 mice in three independent experiments. (*B*) The i.p. tumor challenge in PTEN$^{+/+}$ or PTEN$^{\Delta/\Delta}$ mice using RMA:RMA/S lymphoma cell lines results in the defective recruitment of peritoneal cells at 24 and 48 h. Data are mean ± SEM of $n = 3$–5 mice in three independent experiments. (*C*) Enriched PTEN$^{+/+}$ or PTEN$^{\Delta/\Delta}$ splenic NK cells were adoptively transferred i.v. into syngeneic Rag2$^{-/-}\gamma_c{}^{-/-}$ mice that simultaneously received i.p. RMA:RMA/S (tumor) or PBS (no tumor, control). After 48 h, the peritoneal cavity was flushed and assessed by flow cytometry for the recruitment of YFP$^+$ NK cells. Summary data of mean ± SEM from three independent experiments are shown ($n = 3$ mice). (*D*) RMA/S (10^6 in Matrigel) were implanted into the right flank of PTEN$^{+/+}$ or PTEN$^{\Delta/\Delta}$ mice. After 5 d, tumor plugs were isolated and analyzed for NK cell infiltration by flow cytometric analysis. Data shown are mean ± SEM of two independent experiments of 3–6 mice each. (*E*) B16F10 cells (3×10^5) were injected i.v. into PTEN$^{+/+}$ or PTEN$^{\Delta/\Delta}$ mice. After 2 wk, lungs were isolated and manually counted under a dissecting magnifier. Data summarize two independent experiments, with each point representing an individual mouse.

Similar defects in PTEN$^{\Delta/\Delta}$ NK cell recruitment were observed when mice were implanted with s.c.-injected RMA/S cells, confirming the inability of PTEN$^{\Delta/\Delta}$ NK cells to traffic to peripheral sites of malignancy (Fig. 8*D*). We additionally performed the converse experiment, in which we injected the B16F10 melanoma cell line i.v. into PTEN$^{+/+}$ or PTEN$^{\Delta/\Delta}$ mice. In this model, B16F10 travels via the blood to the lung, forming lung nodules. As expected, we found fewer metastatic lesions in PTEN$^{\Delta/\Delta}$ mice after tumor challenge, likely reflecting the increased NK cell frequency in the lung and peripheral blood (Fig. 8*E*). Taken together, these data implicate PTEN as a critical regulator of NK cell localization during both homeostasis and malignancy.

Discussion

The PI3-kinase pathway plays a central role in NK cell biology; however, the contribution of PTEN as a major negative regulator of this pathway in NK cells was previously unexplored. We hypothesized that selective PTEN loss in NK cells would reveal dominant functional pathways regulated by this phosphatase in vivo. Using a previously unreported mouse model with an NK cell-intrinsic PTEN deletion, our studies demonstrate that PTEN is critical for the appropriate steady-state localization of NK cells in vivo and that PTEN deficiency results in a profound reduction of NK cells in a number of peripheral NK cell compartments, including the major NK cell reservoir—the spleen. PTEN$^{\Delta/\Delta}$ NK cells were hyperproliferative and displayed significant increases in cell death in vivo, resulting in an overall moderate deficiency of NK cells. We note that in these experiments it is difficult to directly compare measures of proliferation and cell survival by simple summation, as both are snapshots of markers associated with proliferating or dying cells and do not fully reflect the kinetics of each process. Given that both increased proliferation and cell death occur and total NK cell numbers are modestly reduced, we take these data to indicate that the increased cell death approximately balances that of proliferation. Therefore, our data suggest that in contrast to PI3K deficiency where NK cell development was profoundly affected (12, 13), lack of PTEN primarily perturbs NK cell localization and cellular turnover, but only modestly affects terminal maturation.

PTEN$^{\Delta/\Delta}$ mice display both a decreased egress of blood NK cells and increased exit of BM NK cells in vivo, which is mechanistically explained by augmented responses to S1P. The predominant S1P receptor in NK cells is $S1P_5$, although the T-cell–centric $S1P_1$ receptor may be minimally expressed (5). We did not detect changes in either $S1P_1$ or $S1P_5$ mRNA transcript level, but this does not exclude changes at the protein level due to endocytosis, degradation, or shedding. Nonetheless, we observed increased S1P migration and signaling responses consistent with a hyperactive S1P receptor. Although we observed increased S1P-induced chemotaxis with peripheral blood and spleen PTEN$^{\Delta/\Delta}$ NK cells, this was not evident with BM PTEN$^{+/+}$ or PTEN$^{\Delta/\Delta}$ NK cells to S1P, likely reflecting the low $S1P_5$ expression on the immature NK cells that make up a large part of the BM (6), and rapid transit of mature NK cells into the blood in PTEN$^{\Delta/\Delta}$ mice.

Our phenotype is also consistent with the proposed role of S1P in NK cell trafficking. S1P concentrations are highest in the peripheral blood and lymph and are important for NK cell exit to these sites (42). $S1P_5{}^{-/-}$ mice display elevated NK cell numbers within the BM and LN due to an inability to sense an effective recruitment signal (4, 5). In the case of enhanced $S1P_5$ signaling, our data imply that NK cells are preferentially retained in the peripheral blood, and NK cells in other organs (such as the spleen) would either be recruited to the peripheral blood or be prevented from entering that organ.

Interestingly, previous work has demonstrated that PI3K activity represses T-cell expression of CD62L through transcriptional and proteolytic mechanisms (43), consistent with our observations of increased PI3K activity and constitutively down-regulated

CD62L on PTEN$^{\Delta/\Delta}$ NK cells. Mechanistically, PI3K/mTOR, through regulation of Foxo1, represses KLF2 activity, resulting in loss of CD62L expression (44). This pathway similarly controls the expression of $S1P_1$ on T cells, and loss of KLF2 results in abated $S1P_1$ expression (45). However, in our model, PTEN deletion and commensurate increased PI3K activity should result in decreased S1P receptor expression. These data imply that PI3K regulation of $S1P_5$ receptor expression in NK cells is different from $S1P_1$ in T cells. Consistent with this, $S1P_5$ down-regulation in NK cells has been shown to be FTY-720 insensitive, in direct contrast to T cells (5, 6).

A previous report has demonstrated that NK cell deletion of the p110δ isoform of PI3K also results in the defective trafficking of NK cells, suggesting that the balance of PI3K signals is critical for normal NK cell distribution (32). However, these PI3K-deficient NK cells are less responsive to numerous chemokines acting through $G_{\alpha i}$, including CXCL12, CCL3, CXCL10, and S1P. In our experiments, we observed increased migration selectively in response to S1P, suggesting that PTEN differentially controls either the expression of $S1P_5$ and/or downstream signals of the S1P receptor. Is this phosphatase regulation of NK cell trafficking specific for PTEN? Mice lacking the alternative $PI(3,4,5)P_3$ phosphatase SHIP1 have no reported defects in NK cell trafficking (17), despite observations that SHIP1, and not PTEN, is the major regulator of neutrophil chemotaxis (20). Although other phosphatases have not yet been evaluated in NK cells, this suggests that PTEN is likely a dominant regulator of NK cell localization and that PTEN has specialized and divergent functional roles in NK cells, distinct from its mode of regulation in related leukocyte lineages.

PI3-kinase knockout mice also display abnormalities in NK cell effector functions, including cytotoxicity and IFN-γ production (11, 12, 14). We demonstrate that PTEN promotes IFN-γ production in response to cytokine stimulation, although the mechanism underlying this effect has not yet been elucidated. From these data, it is clear that PTEN is required for the recruitment of NK cells to a site of tumor challenge and therefore the initial stages of an effective antitumor response. We speculate that this requirement would be applicable to other tumors and infections as well. Given the role of PTEN as a central tumor suppressor gene and its causative role in a number of autosomal dominant disorders, including Cowden syndrome and *Proteus* syndrome (46), it is possible that patients harboring inherited PTEN loss-of-function mutations may also have alterations in NK cell localization and subsequent defects in tumor immunosurveillance.

Collectively, our data suggest that PTEN deletion in NK cells principally affects key events responsible for proliferation, cell survival, and appropriate cell trafficking and distribution in vivo. Because complex mechanisms contribute to the altered in vivo distribution of NK cells in PTEN$^{\Delta/\Delta}$ mice, we expect that future studies of PTEN-deficient NK cells will reveal its importance for NK cell responses to both infection and malignancy.

Materials and Methods

Mice. Ncr1 knock-in iCre mice (25), a kind gift of Dr. Eric Vivier (Centre d'Immunologie de Marseille-Luminy, France), were bred to ROSA26 YFP$^{lox/stop/lox}$ knock-in mice (The Jackson Laboratory, stock no. 006148) and PTEN$^{loxp/loxp}$ mice (The Jackson Laboratory, 006440). For mixed BM chimera experiments, B6.SJL (CD45.1$^+$) recipient mice (The Jackson Laboratory, stock no. 002014) and CD45.1/CD45.2 competitor mice were used. Tg(Ncr1-iCre)265Sxl were obtained from Veronika Sexl (27). All mice were maintained on a C57BL/6 background. In all experiments, PTEN-deficient NK cells were identified during flow cytometric analysis by the concurrent expression of YFP, NK1.1, and NKp46 and lack of CD3. All mice have been bred and maintained in specific pathogen-free housing, and all experiments were conducted in accordance with the guidelines of and with the approval of the Washington University Animal Studies Committee. Mice were used between 8 and 12 wk of age for all experiments.

Antibodies, Cytokines, Flow Cytometry, and Cell Sorting. A list of flow cytometry antibodies is detailed in *SI Materials and Methods*. Cytokines used include IL-12 and IL-15 (Peprotech) and IL-18 (MBL). All flow cytometry data were collected on a Gallios flow cytometer (Beckman Coulter). Collected data were analyzed using FlowJo (Tree Star) or Kaluza (Beckman Coulter) software. Cell sorting was performed on a BD FACS Aria II to greater than 99% purity.

Competitive Adoptive Transfer. Competitive adoptive transfers were performed with isolated splenocytes, BM cells, or peripheral blood cells that were labeled with various membrane and cytoplasmic dyes (PKH26, Sigma; CellVue Claret, Sigma; CellVue Burgundy, eBioscience; CellTrace Violet, Invitrogen) according to the manufacturers' instructions. To account for cell labeling effects, dyes were switched in subsequent experiments. We injected i.v. 3×10^6 total peripheral blood cells (1×10^6 of each genotype), 10×10^6 total BM cells (5×10^6 of each genotype), or 60×10^6 total splenocytes (20×10^6 of each genotype) into a wild-type recipient. In our experiments, BM competitive transfer was performed using wild-type and PTEN$^{\Delta/\Delta}$ cells only. After 16 h, recipient mice were killed and organs processed as described below.

Organ Isolation and Processing. Mice were killed by CO_2 asphyxiation, and organs were isolated immediately. All organs received ammonium–chloride–potassium lysis treatment. Cell counts were obtained by trypan blue exclusion and hemacytometer counting or using propidium iodide exclusion with a Cellometer counter (Nexcelom). In some experiments, flow cytometric cell counting beads (Spherotech) were used. Unless otherwise stated, peripheral blood was isolated by cardiac puncture before harvesting other organs, and in adoptive transfer experiments, lymphocytes were enriched using Histopaque 1077 (Sigma) gradient separation. Liver NK cells were isolated by dissociating whole liver using a tissue grinder. Lymphocytes were isolated using a 1:1 Percoll (GE Healthcare) gradient. To isolate splenocytes, spleens were crushed through a 70-μm filter. To isolate lung NK cells, lungs were minced and placed into serum-free DMEM with 0.7 mg/mL collagenase (Sigma) for 20 min at 37 °C. Dissociated lungs were then crushed through a 70-μm filter. For isolation of BM cells, a single femur was removed and flushed with a 23-gauge needle. LN cells were isolated by removal of both inguinal LNs and crushing through a 70-μm filter. The total BM space was estimated based on the femur occupying 5% of the total marrow content (47). Total blood volume was estimated to be 1.5 mL (48). Total LN content was estimated by multiplying the cell number in both inguinal LNs by 22, the number of identifiable LN pairs in mice (49).

Proliferation and Viability Assays. Mice were injected with 150 μg/mouse BrdU (Sigma) i.p. every 12 h for 3 d before sacrifice and organ harvest. Single cell suspensions from each organ were fixed and permeabilized using the Cytofix/Cytoperm kit (BD), treated with DNase I (30 μg, Sigma) for 1 h at 37 °C, and stained with anti-BrdU antibody (BD) before flow cytometric analysis. Ki-67 staining was assessed using a Ki-67 Set (BD) according to the manufacturer's instructions. To assess early and late apoptosis, single cell suspensions from each organ were resuspended in Annexin V binding buffer (100 mM Hepes, pH 7.4, 140 mM NaCl, 2.5 mM $CaCl_2$) and stained using Annexin V (BD) and 7-AAD (Sigma).

Anti-CD45 Sinusoidal Assay. The CXCR4 antagonist AMD3100 and VLA-4 small molecule inhibitor firategrast were provided by John DiPersio (Washington University, St. Louis). AMD3100 (Plerixafor) was injected s.c. (150 μg/mouse) or firategrast was injected i.v. (3 mg/mouse) into recipient mice 1 h before sacrifice in selected experiments. Five minutes before sacrifice, 1 μg anti-CD45 was injected i.v. into each mouse. Parenchymal NK cells were identified by lack of CD45 staining, whereas sinusoidal NK cells were identified by the presence of CD45 labeling.

Mixed BM Chimeras. We injected i.v. 4×10^6 whole BM cells (1:1 wild-type CD45.1/CD45.2: PTEN$^{\Delta/\Delta}$ CD45.2) from 6-wk-old mice into CD45.1 congenic mice receiving 900 cGy irradiation. After 8 wk, mice were killed and analyzed by proliferation and survival assays as described previously.

Tumor Recruitment Assays. RMA/S and the parental line RMA were maintained in RPMI + 10% (vol/vol) FBS, harvested at log phase, and 5×10^5 1:1 RMA:RMA/S cells were injected i.p. into recipient PTEN$^{+/+}$ or PTEN$^{\Delta/\Delta}$ mice. The peritoneal compartment was flushed after 24 or 48 h, and the recovered cells counted and analyzed by flow cytometry for YFP$^+$ CD3$^-$ NK cells. In separate experiments, 5×10^5 RMA:RMA/S cells were injected i.p. into Rag2$^{-/-}\gamma_c^{-/-}$ mice. Concurrently, enriched donor PTEN$^{+/+}$ or PTEN$^{\Delta/\Delta}$ NK cells (NK Cell Negative Selection Kit II, Miltenyi) were injected i.v. into the tumor-bearing mice. After 48 h, the peritoneal compartment was flushed, processed, and analyzed by flow cytometry. For s.c. RMA/S recruitment experiments,

10^6 RMA/S were mixed with 300 μL growth factor-reduced Matrigel (Corning) and implanted into the right flank of $PTEN^{+/+}$ and $PTEN^{\Delta/+}$ mice. After 5 d, tumor plugs were removed and dissociated in 1 U/mL dispase (Stemcell Technologies), stained for NK cell markers, and analyzed by flow cytometry. B16F10 was maintained in complete DMEM media (10% FBS, 1 mM Hepes, 1 mM nonessential amino acids, 1 mM L-glutamine, 1 mM penicillin/streptomycin). For lung metastases experiments, 3×10^5 B16F10 were injected i.v. into mice. After 2 wk, lungs from challenged mice were removed and fixed in Fekete's solution (70% ethanol, 1.2% formalin, and 4% glacial acetic acid) to facilitate manual counting under a dissecting magnifier.

Transwell Assays. S1P (Sigma), CXCL12, CCL2, CCL3, or CXCL10 (Peprotech) were added to a total of 500 μL of RPMI + 4 mg/mL fatty acid-free BSA (Fisher) in the bottom chamber of 24-well, 5-μm transwell inserts (Corning). S1P was prepared by sonication in methanol and stored in aliquots under nitrogen at –20 °C. Immediately before assays, the methanol was evaporated under nitrogen. The remaining lipid film was redissolved in RPMI + 4 mg/mL fatty acid-free BSA. Splenic, BM, or peripheral blood wild-type (no YFP reporter) or $PTEN^{\Delta/\Delta}$ NK cells were mixed and added to the top transwell chamber at 2×10^6 cells in 100 μL for splenocytes and BM, or 5×10^5 cells for peripheral blood mononuclear cells. The transwell plate was then incubated at 37 °C for 3 h. Each assay contained a no transwell control (input cells) and a chemokine-free transwell (spontaneous migration). Cell counting was performed using flow cytometry and spike-in counting beads (Spherotech).

Statistical Analysis. Two-way ANOVA or a Student's *t* test was used to determine significance where appropriate. All statistical analyses were calculated in GraphPad Prism software and shown as $*P < 0.05$, $**P < 0.01$, $***P < 0.001$.

ACKNOWLEDGMENTS. We thank Anthony French, Marco Colonna, Deepta Bhattacharya, Timothy Ley, and Megan Cooper for insightful discussion. We also thank Dr. John DiPersio for reagents, Bruno Benitez and Matthew Cooper for skilled technical assistance, and Dr. Veronika Sexl for the Ncr1-tg iCre mice. The authors thank the Washington University Pathology and Immunology Cell Sorting Facility and the Siteman Cancer Center Flow Cytometry Core. This work was supported by National Institutes of Health Grants NIH T32 HL708836 (to R.P.S.), K08AI104991 (to B.A.P.), K08HL093299 (to T.A.F.), and R01AI102924 (to T.A.F.) and a Physician-Scientist Early Career Award from the Howard Hughes Medical Institute (to T.A.F.).

1. Yokoyama WM, Kim S, French AR (2004) The dynamic life of natural killer cells. *Annu Rev Immunol* 22(11):405–429.
2. Di Santo JP (2008) Natural killer cells: Diversity in search of a niche. *Nat Immunol* 9(5):473–475.
3. Orange JS, Ballas ZK (2006) Natural killer cells in human health and disease. *Clin Immunol* 118(1):1–10.
4. Mayol K, Biajoux V, Marvel J, Balabanian K, Walzer T (2011) Sequential desensitization of CXCR4 and S1P5 controls natural killer cell trafficking. *Blood* 118(18):4863–4871.
5. Jenne CN, et al. (2009) T-bet-dependent S1P5 expression in NK cells promotes egress from lymph nodes and bone marrow. *J Exp Med* 206(11):2469–2481.
6. Walzer T, et al. (2007) Natural killer cell trafficking in vivo requires a dedicated sphingosine 1-phosphate receptor. *Nat Immunol* 8(12):1337–1344.
7. Grégoire C, et al. (2007) The trafficking of natural killer cells. *Immunol Rev* 220(434):169–182.
8. Ponzetta A, et al. (2013) CX3CR1 regulates the maintenance of KLRG1+ NK cells into the bone marrow by promoting their entry into circulation. *J Immunol* 191(11):5684–5694.
9. Koyasu S (2003) The role of PI3K in immune cells. *Nat Immunol* 4(4):313–319.
10. Song MS, Salmena L, Pandolfi PP (2012) The functions and regulation of the PTEN tumour suppressor. *Nat Rev Mol Cell Biol* 13(5):283–296.
11. Jiang K, et al. (2000) Pivotal role of phosphoinositide-3 kinase in regulation of cytotoxicity in natural killer cells. *Nat Immunol* 1(5):419–425.
12. Tassi I, et al. (2007) p110gamma and p110delta phosphoinositide 3-kinase signaling pathways synergize to control development and functions of murine NK cells. *Immunity* 27(2):214–227.
13. Kim N, et al. (2007) The p110delta catalytic isoform of PI3K is a key player in NK-cell development and cytokine secretion. *Blood* 110(9):3202–3208.
14. Guo H, Samarakoon A, Vanhaesebroeck B, Malarkannan S (2008) The p110 delta of PI3K plays a critical role in NK cell terminal maturation and cytokine/chemokine generation. *J Exp Med* 205(10):2419–2435.
15. Nandagopal N, Ali AK, Komal AK, Lee S-H (2014) The critical role of IL-15-PI3K-mTOR pathway in natural killer cell effector functions. *Front Immunol* 5(April):187.
16. Marçais A, et al. (2014) The metabolic checkpoint kinase mTOR is essential for IL-15 signaling during the development and activation of NK cells. *Nat Immunol* 15(8):749–757.
17. Banh C, Miah SMS, Kerr WG, Brossay L (2012) Mouse natural killer cell development and maturation are differentially regulated by SHIP-1. *Blood* 120(23):4583–4590.
18. Anzelon AN, Wu H, Rickert RC (2003) Pten inactivation alters peripheral B lymphocyte fate and reconstitutes CD19 function. *Nat Immunol* 4(3):287–294.
19. Buckler JL, Walsh PT, Porrett PM, Choi Y, Turka LA (2006) Cutting edge: T cell requirement for CD28 costimulation is due to negative regulation of TCR signals by PTEN. *J Immunol* 177(7):4262–4266.
20. Nishio M, et al. (2007) Control of cell polarity and motility by the PtdIns(3,4,5)P3 phosphatase SHIP1. *Nat Cell Biol* 9(1):36–44.
21. Subramanian KK, et al. (2007) Tumor suppressor PTEN is a physiologic suppressor of chemoattractant-mediated neutrophil functions. *Blood* 109(9):4028–4037.
22. Li Z, et al. (2005) Regulation of PTEN by Rho small GTPases. *Nat Cell Biol* 7(4):399–404.
23. Raftopoulou M, Etienne-Manneville S, Self A, Nicholls S, Hall A (2004) Regulation of cell migration by the C2 domain of the tumor suppressor PTEN. *Science* 303(5661):1179–1181.
24. Heit B, et al. (2008) PTEN functions to 'prioritize' chemotactic cues and prevent 'distraction' in migrating neutrophils. *Nat Immunol* 9(7):743–752.
25. Narni-Mancinelli E, et al. (2011) Fate mapping analysis of lymphoid cells expressing the NKp46 cell surface receptor. *Proc Natl Acad Sci USA* 108(45):18324–18329.
26. Lesche R, et al. (2002) Cre/loxP-mediated inactivation of the murine Pten tumor suppressor gene. *Genesis* 32(2):148–149.
27. Eckelhart E, et al. (2011) A novel Ncr1-Cre mouse reveals the essential role of STAT5 for NK-cell survival and development. *Blood* 117(5):1565–1573.
28. Chiossone L, et al. (2009) Maturation of mouse NK cells is a 4-stage developmental program. *Blood* 113(22):5488–5496.
29. Shi Y, et al. (2008) Cannabinoid 2 receptor induction by IL-12 and its potential as a therapeutic target for the treatment of anaplastic thyroid carcinoma. *Cancer Gene Ther* 15(2):101–107.
30. Barletta KE, et al. (2012) Leukocyte compartments in the mouse lung: Distinguishing between marginated, interstitial, and alveolar cells in response to injury. *J Immunol Methods* 375(1-2):100–110.
31. Anderson KG, et al. (2014) Intravascular staining for discrimination of vascular and tissue leukocytes. *Nat Protoc* 9(1):209–222.
32. Saudemont A, et al. (2009) p110gamma and p110delta isoforms of phosphoinositide 3-kinase differentially regulate natural killer cell migration in health and disease. *Proc Natl Acad Sci USA* 106(14):5795–5800.
33. Shen B, Delaney MK, Du X (2012) Inside-out, outside-in, and inside-outside-in: G protein signaling in integrin-mediated cell adhesion, spreading, and retraction. *Curr Opin Cell Biol* 24(5):600–606.
34. Bernardini G, et al. (2008) CCL3 and CXCL12 regulate trafficking of mouse bone marrow NK cell subsets. *Blood* 111(7):3626–3634.
35. Bajénoff M, et al. (2006) Natural killer cell behavior in lymph nodes revealed by static and real-time imaging. *J Exp Med* 203(3):619–631.
36. Beuneu H, et al. (2009) Dynamic behavior of NK cells during activation in lymph nodes. *Blood* 114(15):3227–3234.
37. Garrod KR, Wei SH, Parker I, Cahalan MD (2007) Natural killer cells actively patrol peripheral lymph nodes forming stable conjugates to eliminate MHC-mismatched targets. *Proc Natl Acad Sci USA* 104(29):12081–12086.
38. Chen S, Kawashima H, Lowe JB, Lanier LL, Fukuda M (2005) Suppression of tumor formation in lymph nodes by L-selectin-mediated natural killer cell recruitment. *J Exp Med* 202(12):1679–1689.
39. Malek RL, et al. (2001) Nrg-1 belongs to the endothelial differentiation gene family of G protein-coupled sphingosine-1-phosphate receptors. *J Biol Chem* 276(8):5692–5699.
40. Im D-S, et al. (2000) Characterization of a novel sphingosine 1-phosphate receptor, Edg-8. *J Biol Chem* 275(19):14281–14286.
41. Niedernberg A, Blaukat A, Schöneberg T, Kostenis E (2003) Regulated and constitutive activation of specific signalling pathways by the human S1P5 receptor. *Br J Pharmacol* 138(3):481–493.
42. Rivera J, Proia RL, Olivera A (2008) The alliance of sphingosine-1-phosphate and its receptors in immunity. *Nat Rev Immunol* 8(10):753–763.
43. Sinclair LV, et al. (2008) Phosphatidylinositol-3-OH kinase and nutrient-sensing mTOR pathways control T lymphocyte trafficking. *Nat Immunol* 9(5):513–521.
44. Kerdiles YM, et al. (2009) Foxo1 links homing and survival of naive T cells by regulating L-selectin, CCR7 and interleukin 7 receptor. *Nat Immunol* 10(2):176–184.
45. Carlson CM, et al. (2006) Kruppel-like factor 2 regulates thymocyte and T-cell migration. *Nature* 442(7100):299–302.
46. Keniry M, Parsons R (2008) The role of PTEN signaling perturbations in cancer and in targeted therapy. *Oncogene* 27(41):5477–5485.
47. Colvin GA, et al. (2004) Murine marrow cellularity and the concept of stem cell competition: Geographic and quantitative determinants in stem cell biology. *Leukemia* 18(3):575–583.
48. Blake JA, Bult CJ, Eppig JT, Kadin JA, Richardson JE; Mouse Genome Database Group (2014) The Mouse Genome Database: Integration of and access to knowledge about the laboratory mouse. *Nucleic Acids Res* 42(Database issue):D810–D817.
49. Van den Broeck W, Derore A, Simoens P (2006) Anatomy and nomenclature of murine lymph nodes: Descriptive study and nomenclatory standardization in BALB/cAnNCrl mice. *J Immunol Methods* 312(1-2):12–19.